Lebensm.-Wiss. u.-Technol., 27, 522–532 (1994)

Simultaneous Determination of Thermal Conductivity and Diffusivity of Foods using a Point Heat Source Probe: A Theoretical Analysis

N. Voudouris and K. Hayakawa*

Department of Food Science, New Jersey Agricultural Experimental Station, Cook College, Rutgers University, P.O. Box 231, New Brunswick, NJ 08903 (U.S.A.)

(Received April 26, 1994; accepted June 8, 1994)

A computerized mathematical model was developed to examine theoretically the applicability of a continuous point heat source method for simultaneous determination of thermal conductivity (k) and thermal diffusivity (α) of foods by developing proper data reduction methods. A probe of composite structure as well as an overall finite contact conductance coefficient between the probe and the food was assumed. Glycerol and agar gel were used as reference materials to obtain a mean effective distance 'r' from the point heat source to the temperature sensor location that is needed in the determination. Estimated k for 15 different foods was in good agreement with values obtained from the literature (2.5% maximum deviation), whereas the agreement for α was reasonably good only for foods with large α values. A small overall thermal contact conductance coefficient introduced an error of 46% in k and 35% in α determination. The minimum food size for accurate determination of thermal transport properties was 22 mm height × 8 mm radius, but was further reduced to 17 mm × 5 mm when the heater dimensions were decreased by a factor of four.

Introduction

The demand for thermal conductivity (k) and thermal diffusivity (α) data has been increasing due to more efficient and accurate numerical simulation techniques and also to the expanded application of these techniques to heat transfer process design and development.

Several methods have been developed for determining the thermal transport properties of foods by analysing the heat conduction equation. The suitability of a particular technique is based on food sample physical characteristics, type of application and required accuracy. Comprehensive reviews of the various methods for predicting food thermal transport properties are available in the literature(1–3).

The line heat source probe method is widely employed due to its short test duration, accuracy, and suitability for small samples. For example, Sweat and Haugh (4) used a line heat source probe (38.1 mm long, 0.81 mm in diameter) to measure the k of small food samples (19 mm in length). Furthermore, a theroretical simulation of water at 10 s showed that k could be measured in samples of 4.2 mm radius (5). No work has been reported on simultaneously determining the minimum allowable sample length and radius of the method. It would be desirable to have a shorter probe for even smaller sample application. However, further size reduction of the probe for smaller food samples is troublesome because it is necessary to maintain a probe of length to diameter ratio greater than 25 and an adequate sample diameter (6). Thermal diffusivity can also be determined directly with the line heat source probe by adding one more temperature sensor close to the heat source (7).

A probe based on completely different design, using a point heat source, could be suitable for thermal transport property measurement of small food samples since probe to food contact is required only at a point heater and since a probe shorter than a line heat source probe would be possible. Most point heat source-related measurement techniques utilized a thermistor as both a heating element and a temperature sensor. Kravets and Larkin (8) used a heat thermistor bead method for the simultaneous determination of k and α food particulates. The thermistor's bead was quickly heated to produce a desired step temperature change above the initial temperature of the test material. Then, the achieved temperature (probe resistance) was maintained constant for a short period of time (30 s) using a control strategy. Thermophysical properties were determined by analysing the thermistor's power dissipation/time data. The minimum allowable particle diameter for accurate thermal transport property measurement was 6 mm when maintaining a sufficiently large sample height. The usefulness of this technique was directly dependent upon bead's radius and thermal conductivity, as well as the quality of the calibration materials. The use of a similar technique for measuring α of food materials was described by Thorne (9). A thermistor was used initially as a pulsed point heat source and then the same thermistor was used as a temperature sensor to measure the rate of dissipation of the introduced heat (30 °C temperature rise), which was a direct function of α. However, the attempt to use a thermistor for determining temperature by the resistance variation not only leads to

* To whom correspondence should be addressed.

0023-6438/94/060522 + 11 $08.00/0

complicated controls to yield constant power, but may also introduce boundary effects during α measurement (10).

It is important to note that no published work describes a method that uses a constant, continuous point heat source, although this simplifies the required instrumentation compared to the above described. Therefore, the objective of the present study was to investigate theoretically the feasibility of using a continuous point heat source probe for simultaneous determination of thermal conductivity and diffusivity by: (a) developing a mathematical model for simulating the thermal response of such a probe; and (b) analysing the simulated temperature data by applying an analytical solution of a linearized heat conduction equation for a point heat source.

Mathematical Model Development

A schematic representation of an assumed model, a point heat source probe and its sample holder, is illustrated in **Figs 1a** and **b** (component dimensions not in proportion). An assumed point heat source probe of length L_{pr} and radius R_{pr} is positioned on the central axis of a cylindrical shell, a sample holder filled with food, with an immersion depth L^6. The point heater is approximated by a cylinder of length L^1 and radius R^1 (**Fig. 1a**). The thermal influence of a temperature sensor is assumed to be negligible as assumed by Karwe and Tong (11). The electrically insulated heater lead wire is supported by a low k rod. The heater-lead wire assembly is placed in a protective cylindrical sheath, a thin wall stainless steel tubing (not shown in **Fig. 1a**). The void space around the heater is filled with high conductivity filling material. The sample holder made of stainless steel is filled with heat-conducting food, the inside height and radius dimensions of the sample holder being H^6 and R^6, respectively and outside dimensions being H^7 and R^7. The sample holder equipped with the probe is placed in a well agitated bath of a heat exchange medium to ensure a uniform temperature distribution in the test material before initiating a simulation run. The heater generates a constant heating rate Q_v (W/m^3) starting at time zero.

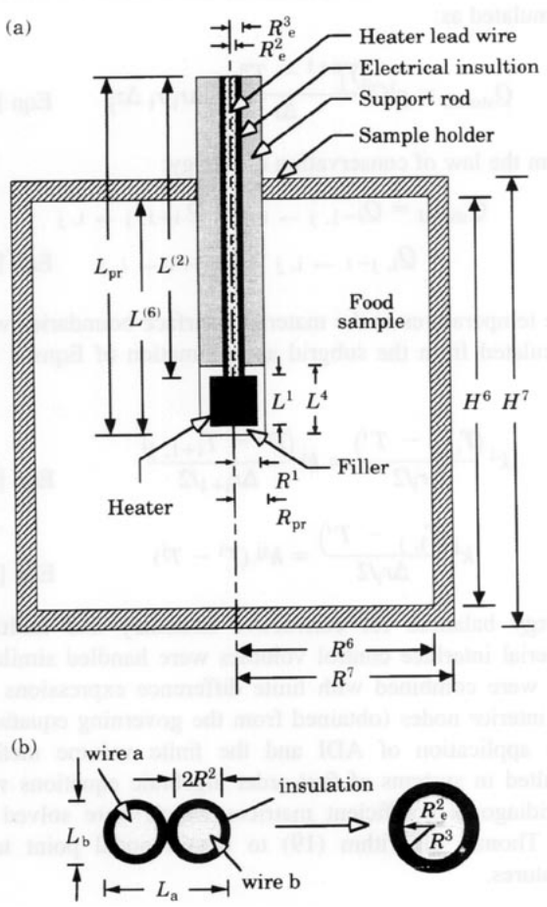

Fig. 1 **a** A cross sectional view of the composite point heat source probe and the sample holder assembly (probe size not in proportion to sample holder); **b** conversion from real heater lead wire to simulation wire radial dimensions

The mathematical representation of the simulation model is governed by a two dimensional heat conduction equation in cylindrical co-ordinates for temperature and location independent material thermophysical properties:

$$\rho^i C^i \frac{\partial T}{\partial t} = \frac{1}{r}\frac{\partial}{\partial r}\left[r\left(k^i \frac{\partial T}{\partial r}\right)\right] + \frac{\partial}{\partial z}\left[\left(k^i \frac{\partial T}{\partial z}\right)\right] + \beta^i Q_v$$

$$(r, z) \in V^i \text{ and } t > 0 \qquad \text{Eqn [1]}$$

Superscript ^{i} denotes different material thermophysical properties and component sizes:

i = 1 for heater
i = 2 for heater lead wire
i = 3 for electrical insulation
i = 4 for high k filler
i = 5 for low k support rod
i = 6 for food sample
i = 7 for sample holder
i = 8 for protective sheath

$\beta^1 = 1$ β^{i}'s for all other materials are nil.

The applicable boundary and initial conditions are shown below.

Boundary conditions. The temperature distribution was assumed to be axisymmetric:

$$\frac{\partial T}{\partial r} = 0$$

$$r = 0,\ (H^6 + H^7)/2 + L_{pr} - L^6 < z < 0 \text{ and } t > 0 \quad \text{Eqn [2]}$$

At the convective boundary:

$$(-1)^p k^i \left.\frac{\partial T}{\partial \vec{n}}\right|^s = h^s (T^m - T^s)$$

$$(r, z) \in S \text{ and } t > 0 \qquad \text{Eqn [3]}$$

When a normal surface vector is in the positive co-ordinate direction, $P = 1$. Otherwise $P = 2$

Conditions on two dissimilar materials interface. The following two equations were included in the model to represent finite contact heat conductance contact conductance:

$$k^i \left.\frac{\partial T}{\partial \vec{n}}\right|^i = k^j \left.\frac{\partial T}{\partial \vec{n}}\right|^j$$

$$(r, z) \in I^{ij} \text{ and } t > 0 \qquad \text{Eqn [4]}$$

$$(-1)^p k^i \left.\frac{\partial T}{\partial \vec{n}}\right|^i = h^{ij} (T^i - T^j)$$

$$(r, z) \in I^{ij} \text{ and } t > 0 \qquad \text{Eqn [5]}$$

$P = 1$ when a normal interface vector from i to j is in the positive co-ordinate direction. $P = 2$ otherwise.

Initial condition.

$$T = T_o$$

$$(r, z) \in (V^i + S) \text{ for all } i \text{ values and } t > 0 \qquad \text{Eqn [6]}$$

$T^m = T_o$ since a thermal conductivity determination test begins after a sample is equilibrated thermally to T^m.

It should be noted that the heater lead wires and their electrical insulation is approximated as a wire of equivalent radius, R^2e, concentrically insulated with an equivalent layer thickness using the following equations as shown in **Fig. 1b** (12):

$$R^3{}_e = (L_a + L_b)/4 \qquad r^2{}_e = \sqrt{2}R^2 \qquad \text{Eqn [7]}$$

The thermal influence of the stainless steel sheath is included in an overall contact conductance:

$$\frac{1}{h^{64}} = \frac{1}{h^{68}} + \frac{l^8}{k^8} + \frac{1}{h^{84}} \qquad \text{Eqn [8]}$$

Numerical Methods

The above set of equations are solved numerically through a hybrid approach applying the alternating direction implicit (ADI) finite difference method (13,14) and the finite volume method (control volume energy balance method (15,16). The ADI method reduces computational time, while maintaining a stable solution (17). The control volume energy balance volume method was applied since finite difference approximations on nodal points located around interfaces, exposed surfaces, and corners are greatly cumbersome to construct.

The solution domain was divided into non-uniformly spaced mesh dimensions in which steep temperature gradients and boundary regions were divided into finer grids. The grid system overlapped the boundaries (the boundary control volumes consist of full volumes next to a boundary) to provide better description at material interface and convective boundaries (13). Nodes were located at the centroid of a control volume. Interfacial thermal conduction was estimated by assuming series conduction paths between adjoining interior node points (18). For adjoining boundary node points, the heat rates were formulated in terms of the corresponding thermal resistances.

Although many types of boundary node arrangement exist, the application of energy balances in a finite volume located next to the interface that separates two dissimilar materials is sufficient to cover all different cases (**Fig. 2**). For this arrangement, the heat rates were expressed as:

$$Q_{i-1,\,j \to i,\,j} = \left[\frac{\left(\frac{\Delta r_{i-1}}{k^i} + \frac{\Delta r_i}{k^i}\right)}{(\Delta r_{i-1} + \Delta r_i)}\right]^{-1} \frac{(T_{i-1,\,j} - T_{i,\,j})}{\left(\frac{\Delta r_{i-1} + \Delta r_i}{2}\right)} \left(r_{i-1} + \frac{\Delta r_{i-1}}{2}\right)\Delta z_j \qquad \text{Eqn [9]}$$

$$Q_{i+1,\,j \to i,\,j} = \left[\frac{\frac{\Delta r_i}{2}}{k^i\left(r_i + \frac{\Delta r_i}{2}\right)\Delta z_j} + \frac{1}{h^{ij}\left(r_i + \frac{\Delta r_i}{2}\right)\Delta z_j} + \frac{\frac{\Delta r_{i+1}}{2}}{k^i\left(r_i + \frac{\Delta r_i}{2}\right)\Delta z_j}\right]^{-1} (T_{i+1,\,j} - T_{i,\,j}) \qquad \text{Eqn [10]}$$

$$Q_{i-1,\,j \to i,\,j} = \left[\frac{\left(\frac{\Delta z_{j-1}}{k^i} + \frac{\Delta z_j}{k^i}\right)}{(\Delta z_{j-1} + \Delta z_j)}\right]^{-1} \frac{(T_{i,\,j-1} - T_{i,\,j})}{\left(\frac{\Delta z_{j-1} + \Delta z_j}{2}\right)} \Delta r_i\, r_i \qquad \text{Eqn [11]}$$

$$Q_{i+1,\,j \to i,\,j} = \left[\frac{\left(\frac{\Delta z_j}{k^i} + \frac{\Delta z_{j+1}}{k^i}\right)}{(\Delta z_j + \Delta z_{j+1})}\right]^{-1} \frac{(T_{i,\,j+1} - T_{i,\,j})}{\left(\frac{\Delta z_j + \Delta z_{j+1}}{2}\right)} \Delta r_i\, r_i \qquad \text{Eqn [12]}$$

The rate of heat accumulation in the control volume was formulated as:

$$Q_{\text{stored}} = \rho^i C^{ij} \frac{T^{n+1}_j - T^n{}_{i,\,j}}{\Delta t} \Delta r_i\, r_i\, \Delta z_j \qquad \text{Eqn [13]}$$

From the law of conservation of energy:

$$Q_{\text{stored}} = Q_{i-1,\,j \to i,\,j} + Q_{i+1,\,j \to i,\,j} + Q_{i,\,j-1 \to i,\,j} + Q_{i,\,j+1 \to i,\,j} \qquad \text{Eqn [14]}$$

The temperatures at the material interface boundaries were calculated from the subgrid approximation of Eqns 4 and 5:

$$k^i \frac{(T_{i,\,j} - T^i)}{\Delta r_i/2} = k^j \frac{(T^j - T_{i+1,\,j})}{\Delta r_{i+1}/2} \qquad \text{Eqn [15]}$$

$$k^i \frac{(T_{i,\,j} - T^i)}{\Delta r_i/2} = h^{ij}(T^i - T^j) \qquad \text{Eqn [16]}$$

Energy balances for convective boundary and multiple material interface control volumes were handled similarly and were combined with finite difference expressions for the interior nodes (obtained from the governing equation). The application of ADI and the finite volume method resulted in systems of first-order algebraic equations with a tridiagonal coefficient matrices which were solved by the Thomas algorithm (19) to obtain nodal point temperatures.

Data Reduction Methods

A data reduction method for a line heat source probe is

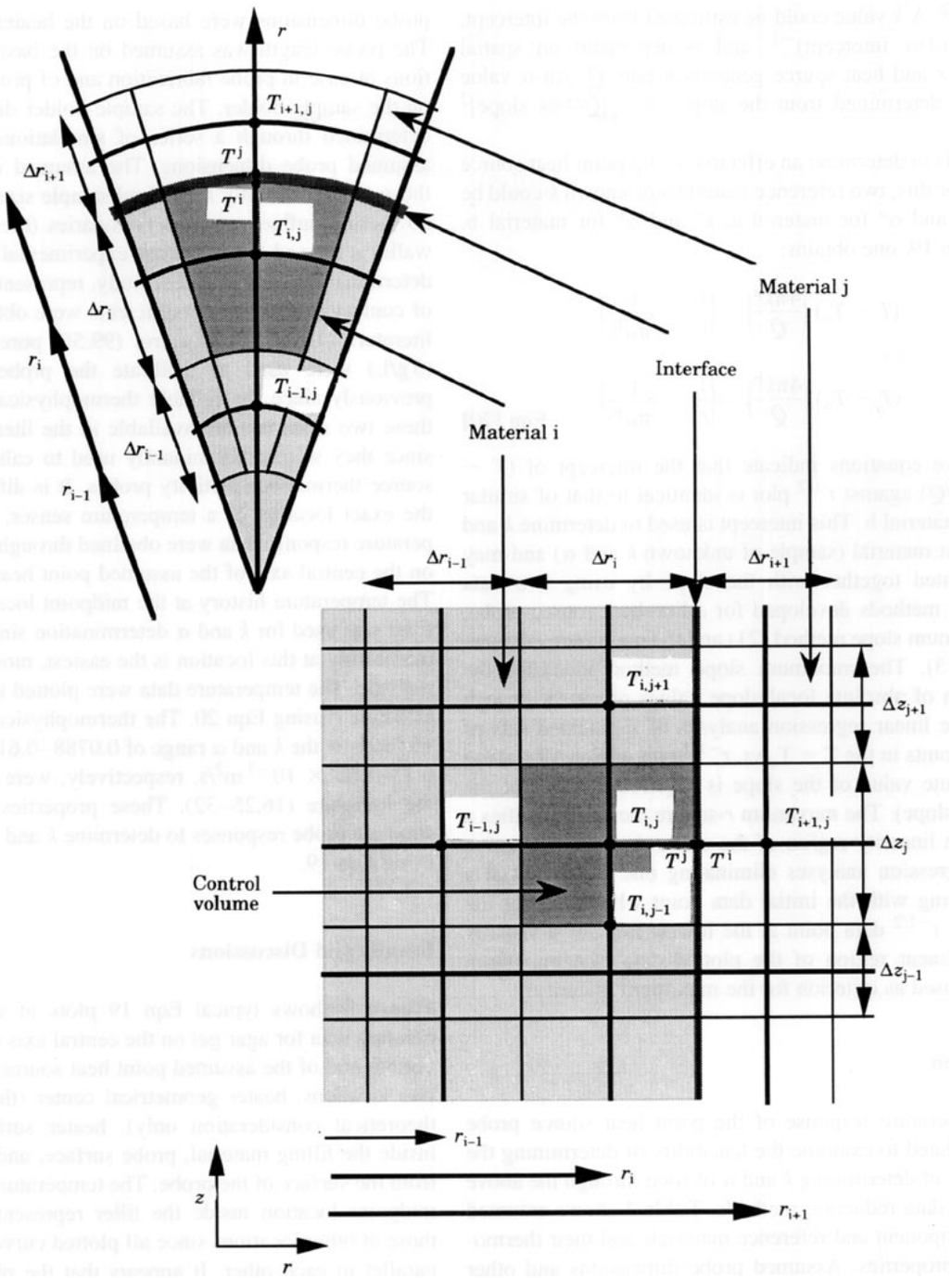

Fig. 2 Application of energy balances in a finite volume located next to the interface that separates two dissimilar materials

based on an analytical solution for heat conduction in an infinite body containing a line heat source of no mass and volume. Following a similar analogy, an analytical solution for a continuous point heat source was used (20) to obtain a data reduction method for temperature data generated by the above described mathematical model:

$$T - T_o = \frac{Q}{4\pi kr} \operatorname{erfc}\left(\frac{r}{\sqrt{4\alpha t}}\right) \qquad \text{Eqn [17]}$$

where,

$$\operatorname{erfc}(x) = 1 - \operatorname{erf}(x) = 1 - \frac{2}{\sqrt{\pi}} \int_o^x e^{-\xi^2} d\xi$$

$$= 1 - \frac{2}{\sqrt{\pi}} \int_o^x \left(1 - \frac{2}{2!}\xi^2 + \frac{12}{4!}\xi^4 - \ldots\right) d\xi$$

$$= 1 - \frac{2x}{\sqrt{\pi}} + \frac{2x^3}{3\sqrt{\pi}} - \ldots \qquad \text{Eqn [18]}$$

In Eqn 17, the value of $r/\sqrt{4\alpha t}$ decreases with increasing t. Therefore, $\operatorname{erfc}(r/\sqrt{4\alpha t})$ may be approximated by the first two terms of Eqn 18 for sufficiently large t values. Thus, one obtains:

$$T - T_o = \left(\frac{Q}{4\pi k}\right)\left(\frac{1}{r} - \frac{1}{\sqrt{\pi\alpha t}}\right) \qquad \text{Eqn [19]}$$

According to Eqn 19, the temperature rise varies linearly

with $t^{-1/2}$. A k value could be estimated from the intercept, $k = Q$ ($4\pi r$ intercept)$^{-1}$, and is dependent on spatial location, r and heat source generation rate, Q. An α value could be determined from the slope, $\alpha = [Q/4\pi k \text{ slope}]^2 \pi^{-1}$.

One needs to determine an effective r of a point heat source probe. For this, two reference materials of known k could be used (k^a and α^a for material a, k^b and α^b for material b. From Eqn 19, one obtains:

$$(T - T_o)\left(\frac{4\pi k^a}{Q}\right) = \left(\frac{1}{r} - \frac{1}{\sqrt{\pi\alpha^b t}}\right)$$

$$(T - T_o)\left(\frac{4\pi k^b}{Q}\right) = \left(\frac{1}{r} - \frac{1}{\sqrt{\pi\alpha^b t}}\right) \qquad \text{Eqn [20]}$$

The above equations indicate that the intercept of $(T - T_o)(4\pi k^a/Q)$ against $t^{-1/2}$ plot is identical to that of similar plot for material b. This intercept is used to determine k and α of a test material (sample of unknown k and α) and may be estimated together with the slope by using two data reduction methods developed for a line heat source probe, the maximum slope method (21) and the maximum r-square method (3). The maximum slope method identifies the maximum of absolute local slope values obtained through successive linear regression analyses of segmented sets of 10 data points in the $T - T_o$ *vs.* $t^{-1/2}$ plot of Eqn 19 (taking the absolute value of the slope is required because of the negative slope). The maximum r-square method identifies a maximum linearity region of the curve through successive linear regression analyses eliminating one data point at a time starting with the initial data point while keeping the minimum $t^{-1/2}$ data point at the lowest limit of a visually selected linear region of the plotted data (the maximum r-square used as criterion for the maximum linearity).

Simulation

The temperature response of the point heat source probe was simulated to examine the feasibility of determining the feasibility of determining k and α of food through the above described data reduction methods. **Table 1** shows assumed probe component and reference materials and their thermophysical properties. Assumed probe dimensions and other model parameter values are listed in **Table 2**. Since an infinitesimally small heat source is physically impossible, the heater was simulated by a small resistor of 3.683 mm length, L^1, and 0.7874 mm radius, R^1 (22). The assumed probe dimensions were based on the heater's dimensions. The probe length was assumed on the basis of considerations of ease in probe fabrication and of probe installement on the sample holder. The sample holder dimensions were determined through a series of simulations based on the assumed probe dimensions. The assumed dimensions are those of a sufficiently large food sample size which ensures no thermal influence on its boundaries (the sample holder walls) at the end of a simulated experimental run for k and α determination. In the present study, representative estimates of contact conductance coefficients were obtained from the literature (16,23,24). Glycerol (99.5% pure) and agar gel (5 g/L) were used to calibrate the probe as described previously since the reliable thermophysical properties of these two materials are available in the literature (16) and since they were predominantly used to calibrate line heat source thermal conductivity probes. It is difficult to define the exact location of a temperature sensor, so probe temperature response data were obtained through the simulation on the central axis of the assumed point heat source probe. The temperature history at the midpoint location inside the filler was used for k and α determination since temperature monitoring at this location is the easiest, most practical and realistic. The temperature data were plotted to determine an effective r using Eqn 20. The thermophysical properties of 15 foods in the k and α range of 0.0788–0.613 W/(mK) and 0.73–1.60 $\times$ 10^{-7} m^2/s, respectively, were obtained from the literature (16,25–32). These properties were used to simulate probe responses to determine k and α of each food using Eqn 19.

Results and Discussions

Figure 3 shows typical Eqn 19 plots of simulated temperature data for agar gel on the central axis and toward the bottom end of the assumed point heat source probe at these five locations, heater geometrical center (this location for theoretical consideration only), heater surface, midpoint inside the filling material, probe surface, and 0.5 mm away from the surface of the probe. The temperature history at the midpoint location inside the filler represented effectively those at other locations since all plotted curves are virtually parallel to each other. It appears that the plot exhibits an approximately linear region, except of an initial curvature of considerable time lag (large $t^{-1/2}$ values region) and a leveling off at late times (small $t^{-1/2}$ values region). The initial departure from the ideal condition is probably due to

Table 1 Properties of probe and reference materials used in simulation

Material	C (J/(kgK))	k (W/(mK))	ρ (kg/ m^3)	α (m^2/s)
Sample holder (Stainless steel)[11]	455	13.8	7917	3.83×10^{-6}
Heater lead wire (Cooper)[16]	385	401.0	8933	1.16×10^{-4}
Reference Material (Agar gel)[16]	4179	0.613	997	1.47×10^{-7}
(Glycerol)[16]	2436	0.2876	1259	9.37×10^{-8}
High k filler[11]	3830	2.38	2380	2.60×10^{-7}
Heater (Constantan)[11]	410	21.8	8900	5.97×10^{-6}
Low k support rod (Nylon)[25]	1700	0.24	1100	1.28×10^{-7}
Electrical insulation (Teflon)[11]	993	0.26	2180	1.20×10^{-7}

Table 2 Probe component and sample holder assembly sizes and other model parameters used in the numerical simulations (values computed through simulations or obtained from the literature)

Parameter	Value
Initial temperature (T_o):	24.0 °C
Convective surface heat conductance (h^s):	5.0×10^2 W/(m^{2}K)
Overall thermal contact conductance for ij = 64 (h^{ij})	$1.0 \times 10^2 - 1.0 \times 10^7$ W/(m^{2}K)
Thermal contact conductance for ij ≠ 64 (h^{ij})	$1.0 \times 10^2 - 1.0 \times 10^5$ W/(m^{2}K)
Point heat source heat generation rate (Q):	0.1 W
Time increment	0.4 s
Food size	
Radius (R^6):	1.6×10^{-2} m
Height (H^6):	3.8×10^{-2} m
Sample holder size	
Radius (R^7):	2.0×10^{-2} m
Height (H^7):	4.6×10^{-2} m
Wall thickness ($R^7 - R^6$ or $(H^7 - H^6)/2$):	4.0×10^{-3} m
Probe size	
Radius[a] (R_{pr}):	1.524×10^{-3} m
Length (L_{pr}):	3.158×10^{-2} m
Probe immersion depth in food (L^6):	2.158×10^{-2} m
Heater size	
Radius (R^1):	7.874×10^{-4} m
Length (L^1):	3.683×10^{-3} m
Heater encapsulation length (L^4):	5.583×10^{-3} m
Heater lead wire size	
Radius[b] (R^2_e):	5.39×10^{-5} m
Length (L^2):	2.695×10^{-2} m
Electrical insulation thickness[b] ($R^3_e - R^2_e$):	1.178×10^{-4} m

[a] Gage 11 tube.
[b] Equivalent radius of heater lead wire, R^2_e and electrical insulation, R^3_e determined from Eqn 7 for a gauge 18 wire (R^2 = 0.076 mm) with insulation thickness ($L_a - 2R^2$ = 0.076 mm).

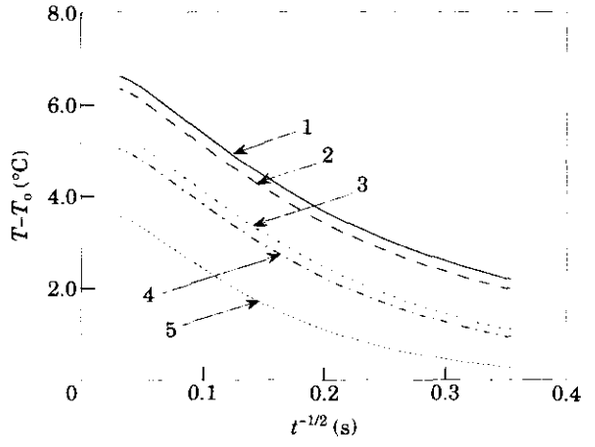

Fig. 3 Typical Eqn 19 plots of simulated temperature data for agar gel on the central axis and toward the bottom end of the assumed point heat source probe at five locations: 1: heater geometrical center, 2: heater surface, 3: midpoint inside filling material, 4: probe surface, and 5: 0.5 mm away from the surface of the probe

the finite mass and volume of the heat source, the difference between the thermal properties of the probe and the test material. Boundary end effects caused the leveling off of the curve. It is also interesting to note that a temperature gradient exists between the heater center and the probe surface in spite of the assumed high conductivity filter. The further away from the heater center, the longer it takes for the curve to reach the region of linearity.

The effective r was determined from the intercept of Eqn 20 using glycerol and agar gel as reference materials and applying the two data reduction methods, the maximum slope and the maximum r-square, as criteria for maximum linearity. **Figure 4** shows sample Eqn 20 plots at the midpoint location inside the filler material for the two reference materials and the effective r determination by the maximum slope method. Ideally, the regressed lines for the reference materials should intersect at the intercept location giving identical effective r. In reality, the application of the maximum slope method gave an effective r of 2.2534 and 2.1414 mm for glycerol and agar gel respectively. When the simulation results were analysed by the maximum r-square method, the effective r was equal to 2.2261 and 2.2150 mm, in good agreement with the maximum slope values. There was about 5% difference in the effective r values of the two reference materials. This may be due to their different thermal response characteristics. The observed time lag is

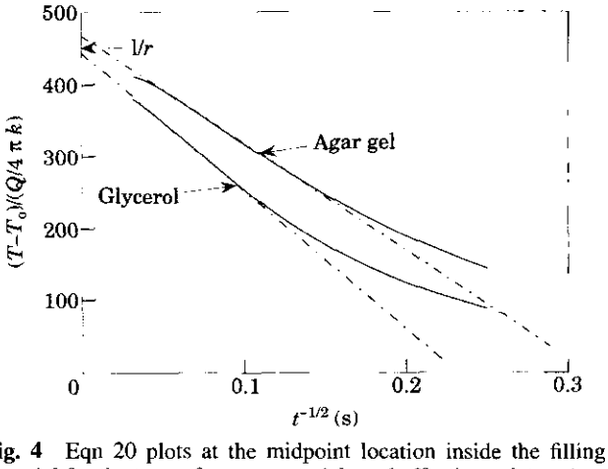

Fig. 4 Eqn 20 plots at the midpoint location inside the filling material for the two reference materials and effective r determination by the maximum slope method

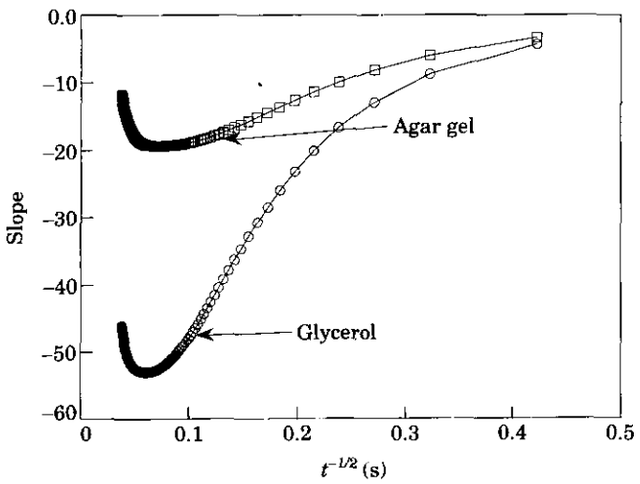

Fig. 5 Theoretical local slope values obtained through successive linear regression analyses of Eqn 19 simulated temperature data at the midpoint location inside the filling material for glycerol and agar gel

about 25 s, longer for glycerol and shorter for agar gels, but is short compared to the overall duration of the simulation run (350 s). Boundary end effects are more profound for agar gel due to its larger α compared to glycerol. A mean effective r is recommended for determining the thermal transport properties of a test material.

The applicability of the maximum slope method to a point heat source was initially investigated by using the mean effective r to determine the thermal transport properties of the two reference materials. The local slopes were estimated through successive linear regression analyses of the simulated temperature data as described previously. **Figure 5** shows changes in local slope values as a function of $t^{-1/2}$ (plot of slopes against the midpoint time of each regression analysis interval). The absolute local slope value increased with time, reached a maximum level, and then decreased. This is in agreement with analogous results reported for a line heat source k probe (21,33). The slope decrease at larger times (smaller $t^{-1/2}$) was attributed to convection and end effects. Due to different thermophysical properties, the maximum absolute slope value, was larger and was reached earlier for glycerol than for agar gel. The k values at the level of maximum absolute slope were 0.2949 and 0.5974 W/(mK) for glycerol and agar gel, respectively, about 2.5% different from the literature values used in the numerical solutions. The α values estimated at the maximum slope were 8.24×10^{-8} (m^2/s) for glycerol and 1.50×10^{-7} for agar gel, 12.0 and 2.3% different from the corresponding literature values. The α values estimated by employing Eqn 19 were less accurate since the errors in k are compounded to an error in α.

The same results were analysed using the r-square method of selecting the best linear slope value. The visually selected lowest $t^{-1/2}$ limit of the linear region of the plotted data was 0.0577. The r-square reached a value of 0.9999 after $t^{-1/2}$ was equal to 0.101 and 0.129 for the glycerol and agar gel, respectively. The estimated k and α values using the mean effective r were 0.2948 (W/(mK)) and 8.50×10^{-8} (m^2/s) for glycerol, and 0.5976 and 1.56×10^{-7} for agar gel, in good agreement with the results obtained using the maximum slope method.

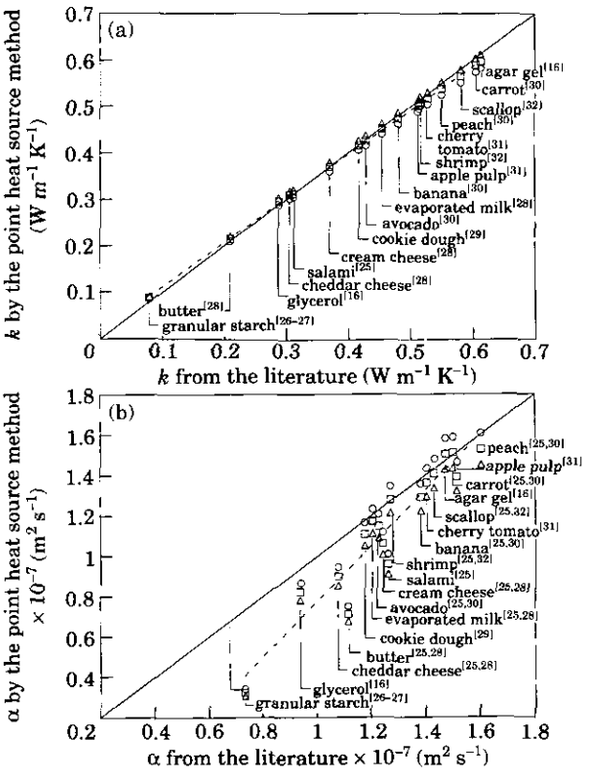

Fig. 6 Comparison of k and α values obtained from the literature with those estimated by the point heat source applying the maximum slope data reduction method for a number of foods. ○, effective r determined using glycerol; △, agar gel; −−⊟−−, mean effective r. **a** k values; **b** α values

Figure 6 summarizes comparative results on the k (**Fig. 6a**) and α (**Fig. 6b**) for 15 different foods. In the figure, the k and α values determined by applying the maximum slope method and using the mean effective r as well as the effective r obtained from each of the two reference materials were plotted *vs.* the literature values. Results obtained by applying the maximum r-square method are not given since they were virtually identical to those obtained by the maximum slope method (0.2% maximum difference). The diagonal line is the 45° line that passes from the origin. k values determined by the point heat source method were in good agreement with those from the literature except for granular starch that gave 12.2, 9.4, and 15% larger k value when using the mean effective r and the r value obtained from glycerol and agar gel, respectively (**Fig. 6a**). It is noted that k and α values of granular starch are way out of the range of glycerol and agar gel values, resulting in inapplicable utilization of effective r for accurate property determination. The coefficient of correlation of the best-fit line (dotted line) by linear regression for the k data was 0.9998. The percent differences between the estimated and literature k using the mean effective, glycerol, and agar gel r were 5.1 for peach, and 5.0% for butter, respectively (peach with the highest α and butter with very low α in the food studied). Similar, but less accurate results were obtained for α (**Fig. 6b**). Best-fit by linear regression for α estimation using the mean effective r gave a coefficient of correlation equal to 0.9474 (dotted line). The largest deviation from the literature α values was observed for granular starch, 55%, followed by butter, 36%, salami, 24%, and cheddar cheese, 16%. The best agreement was observed for scallops and

carrots, 0.8 and 1.8% difference, respectively. Therefore, the point heat source method did not determine accurately the small thermal diffusivities of food. In general, thermal transport properties of food with large k and α values were more accurately estimated using the effective r obtained from agar gel, whereas those with small k and α values by using the effective r from glycerol. The use of the mean r gave the most balanced results as well as the most accurate property values in the range of the two reference materials. Thermal diffusivity determination of food using a point heat source was also attempted by linearizing differently Eqn 17. The test material is subjected to a constant heating period followed by a nil heating period, a gate functional heat generation. The temperature rise during the period of constant heat generation rate ($0 < t \leq t_b$) is given by Eqn 17 ($T = T_{ht}$). The temperature decay of a point heat source after the gate ($t_b < t$) is obtained by applying a superposition theorem (20):

$$T_{ct} - T_o = \frac{Q}{4\pi kr}\left[\text{erfc}\left(\frac{r}{\sqrt{4\alpha t}}\right) - \text{erfc}\left(\frac{r}{\sqrt{4\alpha(t - t_b)}}\right)\right] \quad \text{Eqn [21]}$$

When one takes the ratio of Eqn 21 to Eqn 17 for equal heating and non-heating period t_x, one has:

$$A = \frac{(T_{ct} - T_o)}{(T_{ht} - T_o)}$$

$$= \frac{\frac{Q}{4\pi kr}\left[\text{erfc}\left(\frac{r}{\sqrt{4\alpha(t_b + t_x)}}\right) - \text{erfc}\left(\frac{r}{\sqrt{4\alpha t_x}}\right)\right]}{\frac{Q}{4\pi kr}\text{erfc}\left(\frac{r}{\sqrt{4\alpha t_x}}\right)} \quad \text{Eqn [22]}$$

Combining Eqns 18 and 22 and satisfying the condition $r^2(4\alpha t_x) \ll 1$, the temperature response of a point heat source at moderately long time is expressed by the following data reduction formula:

$$1 - \frac{\sqrt{\frac{t_x}{(t_b + t_x)}}}{A} = \frac{\sqrt{\alpha\pi}}{r}\sqrt{t_x} - 1 \quad \text{Eqn [23]}$$

The logarithmic form of Eqn 23:

$$\text{Log}\left[1 + \frac{1 - \sqrt{\frac{t_x}{(t_b + t_x)}}}{A}\right] = \frac{1}{2}\log t_x + \log\left(\frac{\sqrt{\alpha\pi}}{r}\right) \quad \text{Eqn [24]}$$

According to Eqn 24, a plot of the log of time t_x *vs.* the log of a function of the temperature rise and time is linear and its intercept could be used to calculate the α of a test material when the slope of the curve is equal to 0.5. The effective r could be estimated using the two reference materials in a similar manner as performed with the data reduction of Eqn 19. **Figure 7** shows an Eqn 24 plot of temperature data for glycerol collected at the five locations stated previously. Curves produced through data plotting have no apparent linear regions that are in accordance with Eqn 24. Therefore, the equation may not be used for α determination.

As has been reported (23,34,35), the thermal contact resistance between the probe and the test material may influence significantly thermal transport property determination. **Figure 8a** shows temperature profiles at 300 s with a constant heat generation rate, $Q = 0.1$ W, along the central axis of the sample holder, filled with glycerol, toward the bottom end for different overall thermal contact conductance coefficients (h^{64}). The h^{64} values were assumed to vary from 10^7 W/(m^{2}K), an almost infinite contact conductance as determined by numerical simulations (no interfacial temperature gradient observed), to 10^2 W/(m^{2}K), a rather small contact conductance for many practical applications (23,24). The curves for h^{64} values from 10^7 to 10^4 W/(m^{2}K)

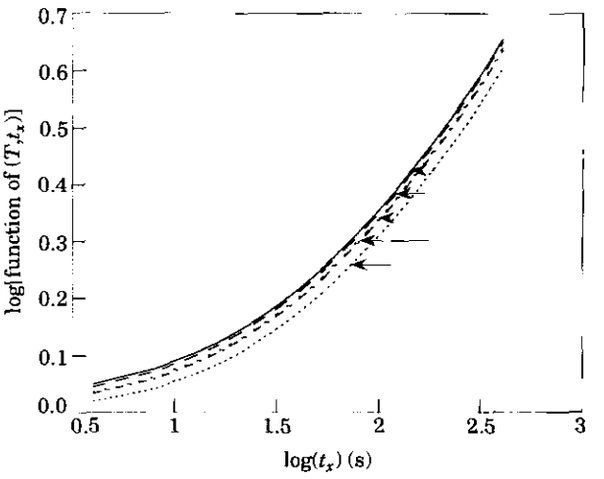

Fig. 7 Eqn 24 plots of simulated temperature data for glycerol at the same five locations as in Fig. 3

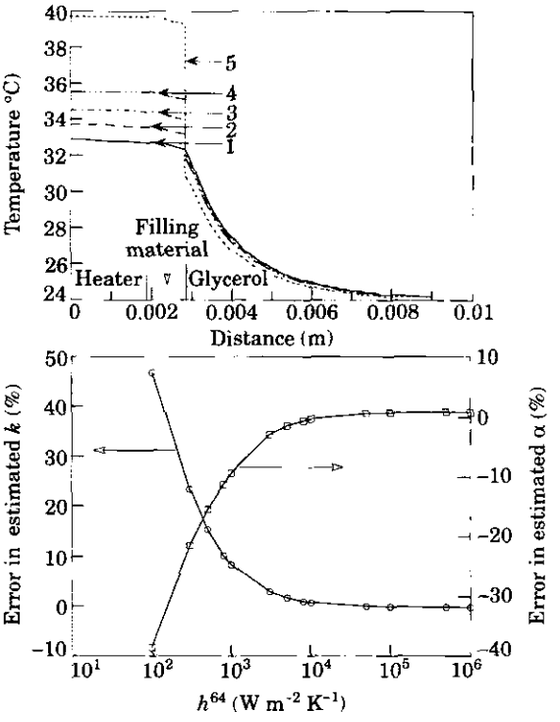

Fig. 8 **a** Temperature profiles at 300 s of constant heat generation rate, $Q = 0.1$ W, along the central axis of the sample holder, filled with glycerol, toward the bottom end for different overall thermal contact conductance coefficients. 1: $h^{64} = 10^7 - 10^4$, 2: $h^{64} = 10^3$, 3: $h^{64} = 5 \times 10^2$, 4: $h^{64} = 3 \times 10^2$, 5: $h^{64} = 10^2$ W/(m^{2}K); **b** error in estimated k and α values of glycerol compared to the literature values *vs.* the logarithm of overall thermal contact conductance. (⊖, k values; ⊟, α values).

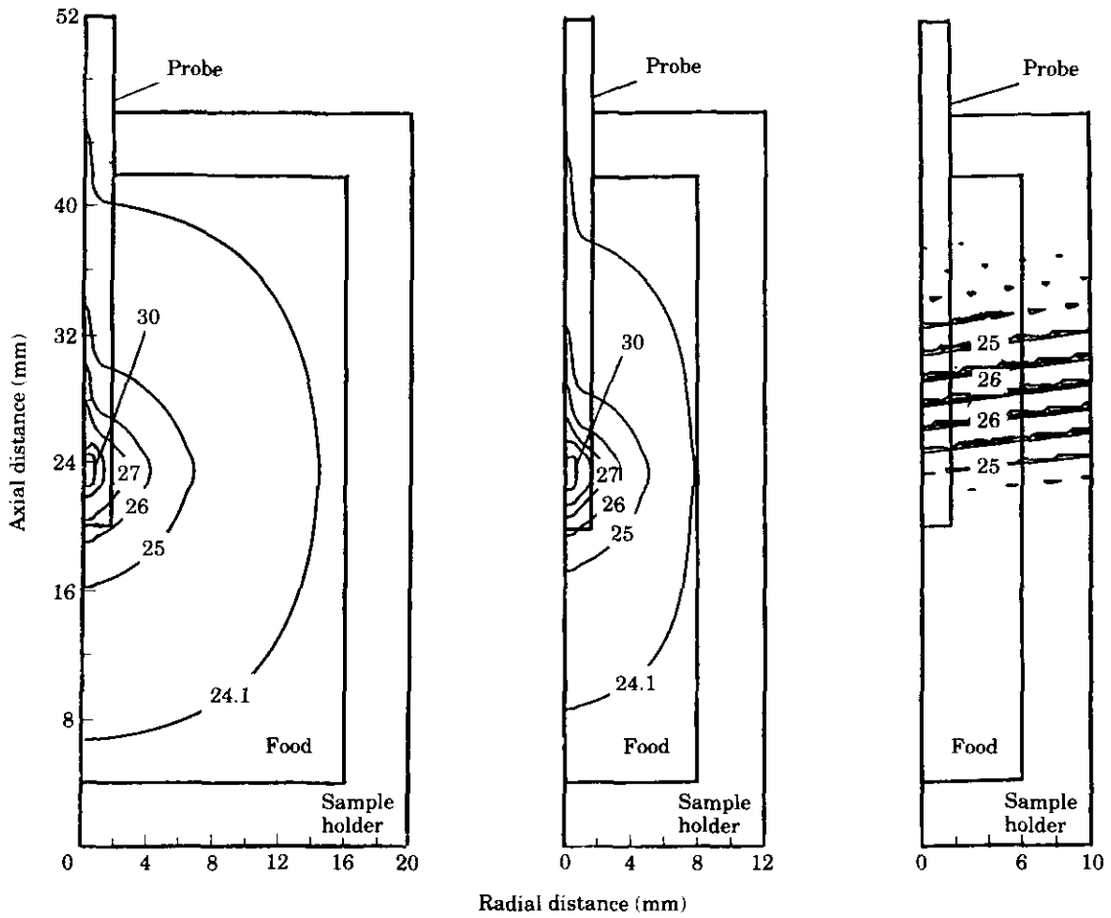

Fig. 9 Computed temperature distributions in one half cross section of the point heat source probe and sample holder assembly for different sample radii, 16, 8, 6 mm, respectively, and identical sample length (agar gel as test material, data collection period of 300 s, Q of 0.1 W, T_0 of 24.0 °C, and h^{64} of 5.0×10^2 W/(m^{2}K)

overlap, implying the minor role of this parameter over the time scales of the simulations. However, any further decrease in h^{64} values resulted in a considerable increase in the temperature drop across the probe–food interface, while the temperature gradient inside the probe remained almost constant (about 0.4–0.5 °C). For an h^{64} of 10^2 W/(m^{2}K) the temperature drop across the interface was 8.5 ° C.

A plot of the error in estimated k and α compared to the literature values *vs.* the logarithm of the thermal conductance is presented in **Fig. 8b**. k and α values were estimated from Eqn 19. The percent of error becomes significant for h^{64} values smaller than 10^{-4} W/(m^{2}K). For example, with an h^{64} of 10^2 W/(m^{2}K) the errors were 46% for the k and 35% for the α.

The major benefit of developing a point heat source for thermal transport property determination is the suitability of the method for foods of small sizes. The minimum sample size may be determined by using the developed simulation model to examine if the sample boundaries experience a temperature change during the longest test time period encountered (2). Therefore, the condition to be satisfied for accurate k and α determination was less than 1% difference between the final and initial temperature of the sample boundary. **Figures 9, a, b** and **c** show computed temperature distributions in one-half cross section of the point heat source probe and sample holder assembly for different sample radii, 16, 8, 6 mm, respectively, and identical sample length. The computer simulations were performed for agar gel as test material, data collection period of 300 s, Q of 0.1 W, T_0 of 24.0 °C, and h^{64} of 5.0×10^2 W/(m^{2}K). For an assumed food radius of 16 or 8 mm (**Figs. 9a, b**), the temperature distribution is not disturbed. However, for a food radius of 6 mm or less (**Fig 9c**), boundary effects take place. The heat wave reaches the boundaries, causing significant errors in thermal transport property determination. Similar simulations were carried out to determine the boundary effect influenced by the sample height. The minimum allowable sample size for the assumed heater size (3.683 mm length × 0.7874 mm radius) was 22 mm height × 8 mm radius. The minimum size of the point heat source method is larger than those of the line heat source probe and heated thermistor bead methods when comparing individually the height and radius of the minimum samples. Continuous point heat source simulation results for a heater of one quarter size of the above assumed, showed faster response time (less than 150 s with the r-square data reduction) and minimum sample size of 17 mm height × 5 mm radius, comparable to the minimum allowable sample size of a line heat source method.

Conclusion

The simultaneous determination of thermal conductivity

and diffusivity of food using a point heat source was analyzed theoretically. The analysis is based on the use of the mathematical model foe simulating the thermal response of a point heat source and of the analytical solution of a linearized heat conduction equation. The model assumes the composite structure of the probe and the effect of the thermal conduct resistance between dissimilar materials. The analysis of the simulation temperature data showed that both the maximum slope and the maximum r-square data reduction methods could be used for estimating k by a point heat source probe. The applicability of the point heat source method depends upon the selection of proper reference materials needed to determine an effective distance r from the point heat source to the temperature sensor. The use of the mean effective r determined by using glycerol and agar gel gave good agreement between estimated and literature k values. The agreement in α results was fair for foods of large α and poor for foods of small α. The effect of thermal contact resistance between the probe and the food on the accuracy of the method was significant when h^{64} values became smaller than 10^4 W/(m^{2}K). The minimum sample size was 22 mm height × 8 mm radius, but it could be significantly smaller when heaters of smaller dimensions are used and/or foods with smaller α values are tested (sample of higher α and lower h^{64} as well as longer collection time increasing the error in k or α determination in small sample sizes).

Further work is needed to study in depth the influence of other key probe parameters such as heater length to diameter ratio, heat generation rate, time interval for regression analysis, convective surface heat conductance coefficient and test period on the accuracy of k and/or α determination before the method is validated experimentally.

Acknowledgement

This paper is based on the work supported in part by the Center for Advanced Food Technology, a New Jersey Commission on Science and Technology Center, U.S. Hatch Act Fund, New Jersey state fund, and mainframe computer time by Rutgers University Computing Services, New Jersey Agricultural Experimental Station publication No. D-10550–2–94 and D-10209–2–94.

Nomenclature

A	Dimensionless temperature as defined $(T_c - T_o)/(T_h - T_o)(-)$
C	Specific heat (J/(kgK))
h^{ij}	Thermal contact conductance coefficient (ij ≠ 64), or overall thermal contact conductance (ij = 64) (W/(m^{2}K))
H	Height (m)
I	Interface between two materials denoted by superscripts (−)
k	Thermal conductivity (W/(mK))
L	Length (m)
L_a	Major diameter of insulated heater lead wires
L_b	Minor diameter of insulated heater lead wires
l	Thickness (m)
$\vec{n}$	Vector normal to interface or exposed surface (−)
p	Constant as defined (−)
Q	Point heat source heat generation rate or heat rate through control volume (W)
Q_{stored}	Rate of heat accumulation in control volume (W)
Q_v	Point heat source heat generation rate (W/m^3)
r	Radial location variable or distance from central axis of point heat source probe (m)
R	Radius (m)
S	Exposed surface
t	Time (s)
t_b	Time at which heat generation is ceased (s)
t_x	Time as defined, t when $t \leq t_b$ or $t - t_b$ when $t > t_b$ (s)
T	Temperature (°C)
T_{ct}	Temperature after terminating heat generation (°C)
T_{ht}	Temperature during point heat generation (°C)
T_o	Initial temperature (°C)
V	Space occupied by material denoted by superscript, excluding interface, or Exposed surface or central axis (−)
x	Dummy variable as defined (−)
z	Axial location variable or distance from bottom of sample holder (m)

Greek symbols

α	thermal diffusivity (m^2/s)
β^i	Heat generation rate factor, 1 for i = 1 and 0 for all other i's (−)
ξ	Dummy variable (−)
ρ	Density (kg/m^3)

Subscripts

e	Equivalent
i	R-directional discretization
j	Z-directional discretization
pr	Probe

Superscripts

a, b, i, j	Material
m	Heat exchange medium
n	Time discretization
1	Heater
2	Heater lead wire
3	Electrical insulation
4	High k filler
5	Low k support rod
6	Food test sample
7	Sample holder
8	Protective sheath
67	Food-sample holder inside wall

64	Food-filler
68	Food-protective sheath
65	Food-support rod
23	Heater lead wire-electrical insulation
14	Heater-filler
15	Filter-support rod
43	Filler-electrical insulation
84	Filler-protective sheath

References

1 NESVADBA, P. Methods for the measurement of thermal conductivity and diffusivity of foodstuffs. *Journal of Food Engineering*. **1**, 93–113 (1982)

2 MOHSENIN, N. N. *Thermal Properties of Food and Agricultural Materials*. New York: Gordon and Breach Science Publishers, p. 83 (1980)

3 MURAKAMI, E. G. AND OKOS, M. R. Measurement and prediction of thermal properties of foods. In: SINGH, P. R. AND MEDINA, A. G. (Eds), *Food Properties and Computer-Aided Engineering of Food Processing Systems*. Boston: Kluwer Academic Publishers, pp. 3–49 (1988)

4 SWEAT, V. E. AND HAUGH, C. G. A thermal conductivity probe for small food samples. *Transactions ASAE*, **17**, 56–58 (1974)

5 MURAKAMI, E. G., SWEAT, V. E., SASTRY, S. K. AND KOLBE, E. Analysis of various design and operating parameters of the thermal conductivity probe. (pers. comm.) (1994)

6 SWEAT, V. E. Thermal properties in foods. In: RAO, M. A. AND RIZVI, S. S. H. (Eds), *Engineering Properties of Foods*. New York: Marcel Dekker Inc., Chap. 1 (1986)

7 NIX, G. H., LOWERY, G. W., VACHON, R. I. AND TANGER, G. E. Direct determination of thermal diffusivity and conductivity with a refined line-source technique. In: HELLER, G. G. (Ed.), *Progress in Astronautics and Aeronautics*. New York: Academic Press, pp. 865–877 (1967)

8 KRAVETS, R. R. AND LARKIN, J. W. Bead thermistor for determination of thermal properties in foods. *ASAE paper* No. 86–6517 (1986)

9 THORNE, S. Local measurement of thermal diffusivity of foodstuffs. In: SINGH, P. R. AND MEDINA, A. G. (Eds), *Food Properties and Computer-Aided Engineering of Food Processing Systems*. Boston: Kluwer Academic Publishers, pp. 113–116 (1988)

10 HOOPER, F. C. AND LEPPER, F. R. Transient heat flow apparatus for the determination of thermal conductivities. *Transactions ASHVE*, **56**, 309–324 (1950)

11 KARWE, M. V. AND TONG, C. H. Effect of filling material on the temperature distribution in a thermal conductivity probe and thermal conductivity measurements: a numerical study. *Journal of Food Processing and Preservation*, **15**, 339–357 (1991)

12 SINGH, B. S. AND DYBBS, A. Error in temperature measurement due to conduction along the sensor leads. *Journal of Heat Transfer*, **98**, 491–495 (1976)

13 DOUGLAS, J., Jr. Alternating direction methods for three space variables. *Numerische Mathematique*, **4**, 41–63 (1962)

14 SMITH, G. D. *Numerical Solution of Partial Differential Equations: Finite Difference Methods* (2nd Edn.) New York: Oxford University Press, p. 37 (1978)

15 TORRANCE, K. E. Numerical methods in heat transfer. In: ROSHENOW, W. M., HARTNETT, J. P. AND GANIC, E. N. (Eds), *Handbook of Heat Transfer Fundamentals*. New York: McGraw-Hill, Chap. 5 (1985)

16 INCROPERA, F. P. AND DE WITT, D. P. *Fundamentals of Heat and Mass Transfer* (3rd Edn.). New York: Wiley, pp. 86, 187, A1 (1991)

17 TRIBAULT, J. Comparison of three dimensional numerical methods for the solution of the heat diffusion equation. *Numerical Heat Transfer* **8**, 281–298 (1985)

18 PATANKAR, S. V. *Numerical Heat Transfer and Heat Flow*. New York: Hemisphere/McGraw-Hill, p. 44 (1980)

19 CARNAHAN, B., LUTHER, H. A. AND WILKES, J. O. *Applied Numerical Methods*. New York: Wiley, p. 454 (1969)

20 CARSLAW, H. S. AND JAEGER, N. C. *The Conduction of Heat in Solids* (2nd Edn). London: Oxford University Press (1959)

21 WANG, J. AND HAYAKAWA, K. Maximum slope method for evaluating thermal conductivity probe data. *Journal of Food Science*, **58**, 1340–1345 (1993)

22 ANONYMOUS. Catalog No. 112. Chicago: Newark Electronics, Chap. 3 (1992)

23 HAYAKAWA, K. AND HWANG, P. M. Apparent thermophysical constants for thermal and mass exchange of cookies undergoing commercial baking processes. *Lebensmittel-Wissenschaft und -Technologie*, **14**, 336–345 (1982)

24 BLACKWELL, J. H. The axial flow error in the thermal conductivity probe. *Canadian Journal of Physics*, **34**, 412–417 (1956)

25 ANONYMOUS. Thermal properties of foods. In: *ASHRAE Handbook Fundamentals* (SI Edn). Atlanta: American Society of Heating, Refrigerating and Air-Conditioning Engineers, p. 30.13 (1993)

26 MAROULIS, Z. B., DROUZAS, A. E. AND SARAVAKOS, G. D. Modeling of thermal conductivity of granular starches. *Journal of Food Engineering*, **11**, 255–271 (1990)

27 DROUZAS, A. E., MAROULIS, Z. B., KARATHANOS, V. T. AND SARAVAKOS, G. D. Direct and indirect determination of the effective thermal diffusivity of granular starch. *Journal of Food Engineering*, **13**, 91–101 (1990)

28 SWEAT, V. E. AND PARMELEE, C. E. Measurement of thermal conductivity of dairy products and margarines. *Journal of Food Process Engineering*, **2**, 187–197 (1978)

29 KULACKI, F. A. AND KENNEDY, S. C. Measurement of the thermo-physical properties of cookie dough. *Journal of Food Science*, **43**, 380–384 (1978)

30 SWEAT, V. E. Experimental values of thermal conductivity of selected fruits and vegetables. *Journal of Food Science*, **39**, 1080–1083 (1974)

31 BHOWMIK, S. R. AND HAYAKAWA, K. A new method for determining the apparent thermal diffusivity of thermally conductive food. *Journal of Food Science*, **44**, 469–474 (1979)

32 MURAKAMI E. G. Effects of thermal processing on the thermal properties of commercial shrimp and scallops. *ASAE Paper* No. 92–6595 (1992)

33 ASHER, G. B., SLOAN, E. D. AND GRABOSKI, M. S. A computer-controlled transient needle-probe thermal conductivity instrument for liquids. *International Journal of Thermophysics*, **7**, 285–294 (1986)

34 VAN LOON, W. K. P., VAN HANEGHEM, I. A. AND SCHENK, J. A. New Model for the non-steady-state probe method to measure thermal properties of porous media. *International Journal of Heat and Mass Transfer*, **32**, 1473–1481 (1989)

35 BHOWMIK, S. R. AND HAYAKAWA, K. In situ determination of apparent thermophysical properties of a composite slab undergoing transient state heat transfer. *Journal of Food Science*, **50**, 1453–1457, 1462 (1985)